International Journal of Solids and Structures 46 (2009) 3009–3017

Contents lists available at ScienceDirect

International Journal of Solids and Structures

journal homepage: www.elsevier.com/locate/ijsolstr

On the calibration of the Chaboche hardening model and a modified hardening rule for uniaxial ratcheting prediction

Mohamad Rezaiee-Pajand *, Sina Sinaie

Department of Civil Engineering, Ferdowsi University of Mashhad, Mashhad, Khorasan Razavi, Iran

ARTICLE INFO

Article history:
Received 24 December 2008
Received in revised form 5 March 2009
Available online 10 April 2009

Keywords:
Cyclic plasticity
Uniaxial ratcheting
Parameter determination
Kinematic hardening
Calibration methods

ABSTRACT

A systematic mathematical approach is developed in the context of uniaxial cyclic ratcheting for the parameter determination of the decomposed Chaboche hardening rule. This is achieved by deriving the relation between the evolution of the backstress and the plastic strain accumulation. Unlike current calibration techniques where a trial–error approach is employed to fit the simulation results to experimental data, the proposed method determines the parameters directly from uniaxial ratcheting experiments. Numerical results indicate that Chaboche's hardening model is much more efficient than what has been demonstrated before. Finally, as an improvement to the decomposed model, a modification is made to one of the backstress components. This improved component enables the model to predict uniaxial ratcheting with more accuracy.

1. Introduction

Ratcheting is defined as the accumulation of plastic strain during cyclic loading in the presence of a mean stress. Many efforts have been made to determine the cyclic characteristics of materials in uniaxial and multiaxial loading. Experiments conducted by Moyar and Sinclair (1963), Benham (1965), Freudenthal and Ronay (1966), Ruiz (1967), Yoshida et al. (1978), Benallal et al. (1989), Hassan et al. (1992), Hassan and Kyriakides (1992, 1994a,b), Yoshida (1995), Delobelle et al. (1995), Corona et al. (1996), Portier et al. (2000), Bocher et al. (2001), Aubin et al. (2003) and Kang et al. (2004) provide data for ratcheting properties of materials. The uniaxial experiments are either stress or strain controlled. Biaxial experiments mostly incorporate stress in one direction (axial tension or internal pressure) and strain in another direction (shear strain or axial strain). One of the best works on uniaxial ratcheting is the experiments conducted by Hassan and Kyriakides (1992) on 1020 and 1026 carbon steels. A set of stress controlled tests were considered in these experiments with focus on the effect of mean stress and stress amplitude on the plastic strain accumulation. Since the work covers a wide range of peak stress values, many researchers have attempted to verify their ratcheting models with these experimental data, for example, Colak (2008) and Dafalias et al. (2008).

Parallel to experiments, various hardening models have been developed to predict the cyclic response of materials using the theory of plasticity. The linear hardening rule proposed by Prager (1956) is the simplest kinematic hardening rule and is capable of representing the Bauscinger effect in cyclic loadings but fails to produce any accumulation of plastic strain in the presence of a mean stress. This is because the stress–strain curves are in the form of closed hysteresis loops. It should be mentioned here that all models which produce a multilinear uniaxial stress–strain relation behave in the same manner and fail to predict ratcheting.

Two main modifications of Prager's hardening rule where introduced afterward. Besseling (1958) and Mroz (1967) suggested the concept of a multisurface model where each surface evolved according to a linear hardening rule. This idea was further pursued by Dafalias and Popov (1974, 1975, 1976) and Krieg (1975) which introduced a two-surface model and later by the bounding surface theory of Dafalias (1986). These hardening rules present a much better response of materials, but alike other multilinear models fail to predict ratcheting.

The other modification to Prager's hardening rule was made by introducing the fading memory of the plastic strain path. This was accomplished by adding the so called "recovery term" to the linear term of Prager's evolution law making the prediction of plastic strain accumulation possible. Initiated by the nonlinear kinematic hardening rule proposed by Armstrong and Frederick (1966), a wide range of kinematic hardening rules have been presented to simulate the ratcheting phenomena using the idea of strain hardening and a recovery term in their equation. Chaboche et al. (1979) and Chaboche (1986) decomposed the backstress into several components where each of the components, individually evolved according to an AF hardening law. The idea of decomposing the backstress has become a main interest since. Chaboche (1991) and Ohno and Wang (1993) later used a modified version of the original AF equation in their decomposed models. Furthermore, in order to improve the uniaxial and multiaxial ratcheting

* Corresponding author. Tel.: +98 915 313 0340.
E-mail address: mrpajand@yahoo.com (M. Rezaiee-Pajand).

0020-7683/$ - see front matter © 2009 Elsevier Ltd. All rights reserved.
doi:10.1016/j.ijsolstr.2009.04.002

simulation, modifications have been made to the Chaboche and Ohno–Wang models by Mcdowell (1995), Jiang and Sehitoglu (1996), Voyiadjis and Basuroychowdhury (1998), Abdelkarim and Ohno (2000), Bari and Hassan (2002), Chen and Jiao (2004) and Chen et al. (2005). A detailed review of various plasticity models used for ratcheting simulation can be found in Chaboche (2008).

An important feature in relation with ratcheting simulation is determining the material parameters used in each hardening model. Little effort has been made to develop a unified strategy for this purpose. Bari and Hassan (2000) divided the uniaxial strain controlled hysteresis curve into segments and related a number of the material constants to each segment. However, some of the parameters where eventually determined by trial and error in order to produce a good fit to the uniaxial hysteresis curve. Koo and Lee (2007) also used a similar approach. Chen and Jiao (2004) took advantage of the monotonic uniaxial tensile curve to determine the material constants. They also used a trial and error method for the determination of some parameters. Hassan et al. (2008) evaluated the parameters using four different experiments, but also ended up using a trial and error method to fit the numerical simulation to the experimental data. The use of either monotonic or the cyclic stress–strain curves is still in controversy. Unfortunately, in many cases, it has been shown that if the parameters of a model are determined by a specific property of the hysteresis loop, the model will fail to simulate other properties efficiently. Moreover, many models are basically developed by uniaxial hysteresis loops, while others are based on biaxial behavior. According to Bari and Hassan (2002) and Chen et al. (2005), no model is yet general enough to simulate both uniaxial and multiaxial ratcheting responses effectively.

The uniaxial experimental data of Hassan and Kyriakides (1992) conducted on CS 1026 are used to confirm the validity of the proposed methods in this paper. A stress controlled test (Fig. 1) is carried out using seven sets of mean stress σ_m, and stress amplitude σ_a given in Table 1. The first three set of experiments vary in the magnitude of the mean stress while having the same stress amplitude, and the other four set of experiments have the same mean stress but differ in the magnitude of the stress amplitude.

2. Description of hardening plasticity models

Commonly used plasticity models for ratcheting simulation possess similar main features. These models are based on the von-Mises yield criteria and a kinematic hardening rule.

The von-Mises criteria is defined as:

$$f(\sigma - \alpha, k) = \sqrt{(s - a) \cdot (s - a)} - k = 0 \tag{1}$$

where s is the deviatoric stress tensor, a is the deviatoric backstress tensor indicating the center of the yield surface and $k = \sqrt{2/3}\sigma_o$ is the size of the yield surface which will be constant in a kinematic hardening model. The dot "·" indicates the inner product as $a \cdot b = a_{ij}\, b_{ij}$. For mathematical convenience, $s - a$ will be further denoted by $\bar{s}$.

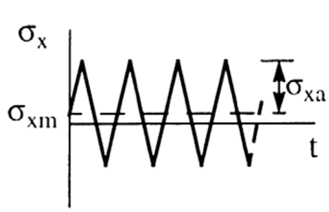

Fig. 1. Uniaxial loading history.

Table 1
Mean stress and stress amplitudes used by Hassan and Kyriakides (1992) for CS1026.

Test No.	1	2	3	4	5	6	7
σ_m (MPa)	28.8	45.0	63.0	44.8	44.8	44.8	44.8
σ_a (MPa)	220.6	220.6	220.6	195.1	209.3	221.5	229.5

The flow rule establishes the direction of the plastic flow. Assuming an associated flow rule in J_2 plasticity, the plastic strain increments will be in the direction of the gradient of the yield surface:

$$d\varepsilon^p = d\lambda \frac{\partial f}{\partial \sigma} = d\lambda \frac{\bar{s}}{\sqrt{2\bar{J}_2}} \tag{2}$$

where $d\lambda$ is called the plastic multiplier and is determined by the consistency condition and $\sqrt{2\bar{J}_2} = \sqrt{\bar{s} \cdot \bar{s}}$.

In order to accommodate hardening effects, a hardening rule is incorporated in the model. Among all hardening rules available, the kinematic hardening rule is the most favorite for ratcheting simulations. This hardening rule governs the evolution of the backstress denoted by a in Eq. (1). As stated in before, various hardening rules have been proposed for hardening and ratcheting simulation. The Armstrong–Frederick hardening rule is an original form which has been modified by many researchers for improved cyclic ratcheting simulation. This model and the decomposed model of Chaboche considered in this study will be briefly discussed here. Detailed characteristics of these models can be found in Bari and Hassan (2000, 2002).

2.1. The Armstrong–Frederick nonlinear hardening model

Armstrong and Frederick (1966) added a recovery term to the linear hardening rule of Prager and proposed a nonlinear hardening rule in the following form:

$$d\alpha = \frac{2}{3} B d\varepsilon^p - \gamma\alpha\sqrt{\frac{2}{3} d\varepsilon^p d\varepsilon^p} \tag{3}$$

The added term, takes into account a fading memory of the plastic strain path. Starting with a plastic modulus of $B \mp (3/2)\gamma\alpha$ in a uniaxial loading condition, α_x eventually stabilizes at a value of $(2/3)B/\gamma$. Incorporating the recovery term was a major development eliminating the deficiencies of linear and multilinear hardening rules. Uniaxial ratcheting can be simulated by this model. However, since few material constants are available to produce an acceptable shape of the stress–strain curve, the AF model is no longer considered suitable for ratcheting prediction.

2.2. The nonlinear hardening rules of Chaboche

Chaboche et al. (1979) and Chaboche (1986) proposed their decomposed hardening rule in the following form:

$$d\alpha = \sum d\alpha_i, \qquad d\alpha_i = \frac{2}{3} B_i d\varepsilon^p - \gamma_i \alpha_i \sqrt{\frac{2}{3} d\varepsilon^p d\varepsilon^p}, \quad i = 1, 2, 3 \tag{4}$$

where each component has the form of an AF type rule. By increasing the material parameters of the hardening rule, the Chaboche model is able to simulate a more accurate prediction of ratcheting than the AF model. However, numerical examples indicate that the model is definitely not suitable for multiaxial ratcheting predictions. The use of three components ($i = 1,2,3$) is suggested by researchers to predict acceptable ratcheting predictions, but as will be established later, utilizing four components will be more precise.

As stated earlier, a systematic method for the determination of material constants of kinematic hardening models has not been developed yet. A general mathematical approach will be established for the decomposed Chaboche model in the following sections. The results indicate that if the material constants of the model are mathematically determined, the accuracy of the original

Chaboche model is much more than what has been claimed in previous papers. For the development of the mathematical procedure, the AF model is initially considered as a preliminary for the more complex method given later.

3. Parameter determination of the Armstrong–Frederick hardening rule

The AF hardening rule is described as in Eq. (3), which takes the following form for uniaxial loading:

$$d\alpha_x = \frac{2}{3}Bd\varepsilon_x^p - \gamma\alpha|d\varepsilon_x^p| \tag{5}$$

The solution of Eq. (5) is as follows:

$$\begin{cases} \alpha_x = \frac{2}{3}\frac{B}{\gamma} + \left(\alpha_{xo} - \frac{2}{3}\frac{B}{\gamma}\right)\exp\left[-\gamma(\varepsilon_x^p - \varepsilon_{xo}^p)\right], & d\varepsilon_x^p \geqslant 0 \\ \alpha_x = -\frac{2}{3}\frac{B}{\gamma} + \left(\alpha_{xo} + \frac{2}{3}\frac{B}{\gamma}\right)\exp\left[\gamma(\varepsilon_x^p - \varepsilon_{xo}^p)\right], & d\varepsilon_x^p < 0 \end{cases} \tag{6}$$

Solving Eq. (6) for ε_x^p, the accumulated plastic strain can be determined for one cycle of loading as given below:

$$\Delta\varepsilon_x^p = \frac{1}{\gamma}\ln\left[\frac{(\alpha_n)^2 - \left(\frac{2}{3}\frac{B}{\gamma}\right)^2}{(\alpha_p)^2 - \left(\frac{2}{3}\frac{B}{\gamma}\right)^2}\right] \tag{7}$$

where α_p and α_n are the maximum and minimum values of the backstress during positive and negative loading, respectively. If however both α_p and α_n attain a same value in a cycle, the term inside the bracket becomes unity and the net plastic strain increment will be zero for that cycle. This will be the case where no mean stress is present during the loading ($\sigma_m = 0$) or when a decomposition of the backstress is used for the hardening model and the backstress components stabilize due to a small value of B_i/γ_i.

For the von-Mises yield criteria along with the associated flow rule, the increments of the backstress tensor take place in the deviatoric plane, therefore, $\alpha_y = \alpha_z = -(1/2)\,\alpha_x$. Referring to the definition of the yield criteria (Eq. (1)), the relation between stress and backstress during uniaxial loading is $|\sigma_x - (3/2)\alpha_x| = \sigma_o$, which by introducing into Eqs. (6) and (7), the following relations can be written:

$$\begin{cases} \sigma_x = \sigma_o + \left[\frac{B}{\gamma} + \frac{3}{2}\left(\alpha_{xo} - \frac{2}{3}\frac{B}{\gamma}\right)\exp\left[-\gamma(\varepsilon_x^p - \varepsilon_{xo}^p)\right]\right], & d\varepsilon_x^p \geqslant 0 \\ \sigma_x = -\sigma_o + \left[\frac{B}{\gamma} - \frac{3}{2}\left(\alpha_{xo} + \frac{2}{3}\frac{B}{\gamma}\right)\exp\left[\gamma(\varepsilon_x^p - \varepsilon_{xo}^p)\right]\right], & d\varepsilon_x^p < 0 \end{cases} \tag{8}$$

and

$$\Delta\varepsilon_x^p = \frac{1}{\gamma}\ln\left[\frac{(\sigma_m - \sigma_a + \sigma_o)^2 - \left(\frac{B}{\gamma}\right)^2}{(\sigma_m + \sigma_a - \sigma_o)^2 - \left(\frac{B}{\gamma}\right)^2}\right] \tag{9}$$

where σ_m is the mean and σ_a is the amplitude of the axial stress cycle. Eq. (9) indicates that the AF hardening model can only produce steady state ratcheting. This equation along with Eq. (6) can be used as a simple calibrating formula for the AF model.

4. Parameter determination of Chaboche's decomposed hardening rule

The hardening rule of Chaboche is defined by Eq. (4). Implementing the same methodology as before, it can be demonstrated that Eqs. (6) and (7) hold for each component of the backstress, therefore the following relations can be written:

$$\begin{cases} \alpha_{ix} = \frac{2}{3}\frac{B_i}{\gamma_i} + \left(\alpha_{ixo} - \frac{2}{3}\frac{B_i}{\gamma}\right)\exp\left[-\gamma_i(\varepsilon_x^p - \varepsilon_{xo}^p)\right], & d\varepsilon_x^p \geqslant 0 \\ \alpha_{ix} = -\frac{2}{3}\frac{B_i}{\gamma_i} + \left(\alpha_{ixo} + \frac{2}{3}\frac{B_i}{\gamma_i}\right)\exp\left[\gamma_i(\varepsilon_x^p - \varepsilon_{xo}^p)\right], & d\varepsilon_x^p < 0 \end{cases} \tag{10}$$

and

$$\begin{cases} \Delta\varepsilon_x^p = -\frac{1}{\gamma_i}\ln\left[\frac{\alpha_{ixp} - \frac{2B_i}{3\gamma_i}}{\alpha_{ixn} - \frac{2B_i}{3\gamma_i}}\right] & \text{(positive phase)} \\ \Delta\varepsilon_x^p = \frac{1}{\gamma_i}\ln\left[\frac{\alpha_{ixn} + \frac{2B_i}{3\gamma_i}}{\alpha_{ixp} + \frac{2B_i}{3\gamma_i}}\right] & \text{(negative phase)} \end{cases} \tag{11}$$

where α_{ip} and α_{in} are, respectively, the maximum and minimum values of the backstress component during positive and negative loading. By dividing a loading cycle and the corresponding plastic strain into a positive phase ($\Delta\varepsilon_x^p > 0$) and a negative phase ($\Delta\varepsilon_x^p < 0$) and assuming that each phase enters the plastic region, the following conditions will be valid:

$$\begin{cases} \alpha_{xp} = \sum \alpha_{ixp} = \frac{2}{3}(\sigma_x - \sigma_o) & \text{(positive phase)} \\ \alpha_{xn} = \sum \alpha_{ixn} = \frac{2}{3}(\sigma_x + \sigma_o) & \text{(negative phase)} \end{cases} \tag{12}$$

Combining Eqs. (10) and (12) will result the following relations:

$$\begin{cases} \alpha_{xp} = \sum\left[\frac{2}{3}\frac{B_i}{\gamma_i} + \left[\alpha_{ixn} - \frac{2}{3}\frac{B_i}{\gamma_i}\right]\exp\left[-\gamma_i\Delta\varepsilon_x^p\right]\right] & \text{(positive phase)} \\ \alpha_{xn} = \sum\left[-\frac{2}{3}\frac{B_i}{\gamma_i} + \left[\alpha_{ixp} + \frac{2}{3}\frac{B_i}{\gamma_i}\right]\exp\left[\gamma_i\Delta\varepsilon_x^p\right]\right] & \text{(negative phase)} \end{cases} \tag{13}$$

Eq. (13) can be used to calibrate the material constants (B_i, γ_i) of a decomposed hardening rule. A set of equations can be attained by using know states of ($\alpha_{ixn}, \alpha_{ixp}, \Delta\varepsilon_x^p$). Different cases of the parameter determination procedure will be discussed in the following sections. These cases will be developed in sequence until an efficient model is obtained.

4.1. One nonlinear component and one linear attachment component (N1-L1)

In the first case a two-component hardening rule composed of one nonlinear and one linear component is considered ($i = 1, 2$ and $\gamma_2 = 0$). If the hardening rule only consisted of one component, the model would lead to a steady state ratcheting case. However, a linear component also exists and its magnitude (α_2) tends to increase as the accumulated plastic strain increases. Since the maximum and minimum values of the backstress are constant (α_p and α_n), this leads to the limitation of the maximum and minimum attainable values of $\alpha_{1p} = \alpha_p - \alpha_2$ and $\alpha_{1n} = \alpha_n - \alpha_2$, respectively. This process will continue until $|\alpha_p - \alpha_2| = |\alpha_n - \alpha_2|$ and there would further be no accumulation of plastic strain.

For the calibration procedure, the material constants of the nonlinear component α_1, are evaluated first. To achieve this, the plastic strain increments of the positive and negative phase of the first cycle are introduced into Eq. (11) and the equation is solved for B_1, γ_1. Next, the plastic strain accumulation of the kth cycle is considered. The magnitude of the linear component of the backstress is denoted by $(\alpha_2)_k$ and by using Eq. (13) the following relation can be written:

$$(\Delta\varepsilon_x^p)_k = (\Delta\varepsilon_{xp}^p)_k + (\Delta\varepsilon_{xn}^p)_k = -\frac{1}{\gamma_1}\ln\left[\frac{(\alpha_p - (\alpha_2)_k) - \left(\frac{2}{3}\frac{B_1}{\gamma_1}\right)}{(\alpha_n - (\alpha_2)_k) - \left(\frac{2}{3}\frac{B_1}{\gamma_1}\right)}\right] + \frac{1}{\gamma_1}\ln\left[\frac{(\alpha_n - (\alpha_2)_k) + \left(\frac{2}{3}\frac{B_1}{\gamma_1}\right)}{(\alpha_p - (\alpha_2)_k) + \left(\frac{2}{3}\frac{B_1}{\gamma_1}\right)}\right] \tag{14}$$

Solving the above equation for $(\alpha_2)_k$ and knowing the total accumulated plastic strain after k cycles, leads to the determination of B_2 by using Eq. (4) with $\gamma_2 = 0$.

Using results of Hassan and Kyriakides (1992) for the experiments conducted on CS 1026, the following values have been obtained by implementing the abovementioned procedure:

$E = 181,300$ MPa, $\quad \nu = 0.302, \quad \sigma_y = 186.2$ MPa
$B_1 = 62,750$ MPa, $\quad \gamma_1 = 552.5$
$B_2 = 1250$ MPa

Fig. 2 compares the predictions of the model with experimental values. This figure shows the value of plastic strain at the positive stress peak of every cycle. The parameters are calibrated for exp2 indicated in the figure.

It is evident from Fig. 2 that the obtained material constants can produce a very good fit to exp1 which they where calibrated for. However, the main shortcoming of the model for other tests is the value of plastic strain in the first cycle. Adding more components to the backstress can overcome this deficiency.

4.2. Three nonlinear components and one linear attachment component (N3-L1)

By utilizing more backstress components, a more precise curve of $\alpha_x - \varepsilon_x^p$ can be attained. This can be accomplished by writing Eq. (13) for more known states of $\alpha_x - \varepsilon_x^p$. However, when multiple components are present, direct use of Eq. (13) is not applicable for two reasons. Firstly because, experimental data can only be used to determine the values of α_x and not its components (α_{ixn} and α_{ixp}). Secondly, solution of a multi-set nonlinear equation in the form of Eq. (13) involves great complexity.

In order to overcome the first problem, Eq. (13) is rewritten in the following form where the terms including α_{ixn} and α_{ixp} are transferred to the left side of the equation:

$$\begin{cases} \alpha_{xp} - \sum \alpha_{ixn} \exp[-\gamma_i \Delta\varepsilon_x^p] = \sum \left[\frac{2}{3}\frac{B_i}{\gamma_i} + \left[-\frac{2}{3}\frac{B_i}{\gamma_i}\right] \exp[-\gamma_i \Delta\varepsilon_x^p]\right] & \text{(positive phase)} \\ \alpha_{xn} - \sum \alpha_{ixp} \exp[\gamma_i \Delta\varepsilon_x^p] = \sum \left[-\frac{2}{3}\frac{B_i}{\gamma_i} + \left[+\frac{2}{3}\frac{B_i}{\gamma_i}\right] \exp[\gamma_i \Delta\varepsilon_x^p]\right] & \text{(negative phase)} \end{cases} \quad (15)$$

In the above equation, if the values of γ_i, α_{ixn} and α_{ixp} on the left side are somehow to be suitably chosen, the terms of the right side of the equations can directly be obtained by experimental data. Calculations show that appropriate values of γ_i, α_{ixn} and α_{ixp} can be effectively evaluated using the method discussed in Section 4.1.

The solution to the second deficiency of solving a nonlinear set of equations in the form of Eqs. (13) and (15) is to predefine the values of $\frac{2}{3}(B_i/\gamma_i)$ and only consider the values of γ_i as unknowns. Although this would increase the number of required components for an acceptable curve fit, but reproduces the set of nonlinear equations to a more easily solved form. The solution process is discussed in the Appendix.

Using results of Hassan and Kyriakides (1992) for the experiments conducted on CS 1026, the following values have been obtained by implementing the abovementioned procedure:

$E = 181,300$ MPa, $\quad \nu = 0.302, \sigma_y = 186.2$ MPa
$B_1 = 56,330$ MPa, $\quad \gamma_1 = 680.9$
$B_2 = 8710$ MPa, $\quad \gamma_2 = 841.7$
$B_3 = 1100$ MPa, $\quad \gamma_3 = 35.5$
$B_4 = 1100$ MPa

It should be noted that the value of B_4 for the linear component is determined using the same method described in Section 4.1.

Fig. 3a and b compares the predictions of the model with experimental values of the plastic strain at positive peak stresses of each cycle. The parameters are calibrated using the curve of exp2 and the plastic strain in the first cycle of exp3.Fig. 3c and d shows the predictions obtained by Bari and Hassan (2000) with the three component Chaboche model (C-H3). Fig. 3e and f is the results obtained by Bari and Hassan (2000) using the four component Chaboche model with threshold (C-H4T). The C-H3 model consists of three AF components in the form of Eq. (4). The C-H4T model is composed of three AF components and takes advantage of one modified AF component. This modified AF component utilizes a threshold for the activation of the recovery term of Eq. (3). More details on these models can be found in Bari and Hassan (2000, 2002).

In order to investigate more characteristics of the suggested calibration technique, Figs. 4 and 5 are presented. Fig. 4 compares the N3-L1 and C-H4T models on their response to a strain controlled hysteresis loop. As can be seen in this figure, the C-H4T model has a slightly better fit to the experimental curve. The reason is that the calibration method suggested by Bari and Hassan (2000) makes direct use of this hysteresis curve to determine the parameters of the model. Fig. 5 exclusively demonstrates the difference between the calibration methods suggested in this paper and by Bari and Hassan (2000). This figure shows the development of plastic strain in a partial reverse loading/reloading stress controlled cycle. It is evident that the C-H4T model traces the $\sigma_x - \Delta\varepsilon_x^p$ curve more closely than the N3-L1 model, however, the total plastic strain accumulated in the cycle is more accurately predicted by the N3-L1 model. These different responses are due to the different strategies and purposes of each parameter determination technique, whereby Bari and Hassan (2000) calibrate the model mainly on the strain controlled hysteresis loop, the present work focuses on the accumulation of plastic strain in nonsymmetric loading cycles.

5. An additional example

Another calibration example has also been prepared for demonstration. Three sets of experiments carried out by Hassan and Kyriakides (1992) on a different material (CS 1020) are considered

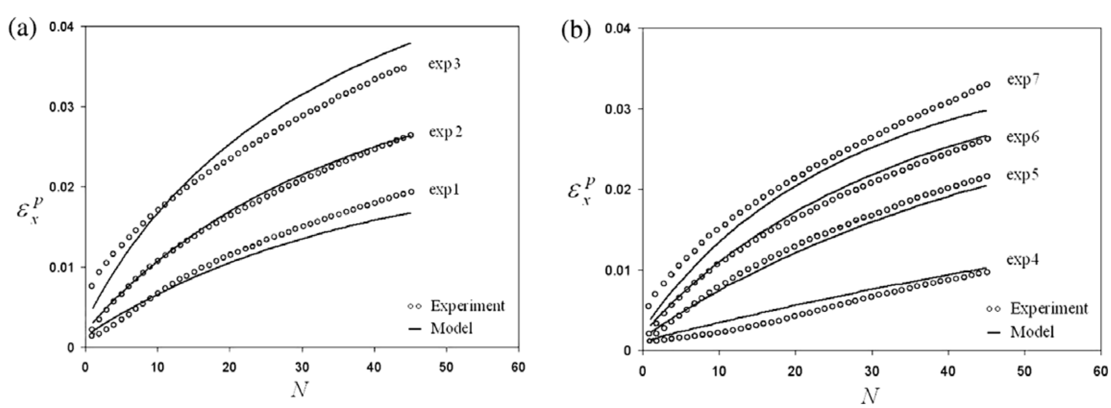

Fig. 2. Comparison of the N1-L1 model with experimental data from Hassan and Kyriakides (1992) for axial plastic strain at positive stress peaks. (a) Experiments 1–3. (b) Experiments 4–7.

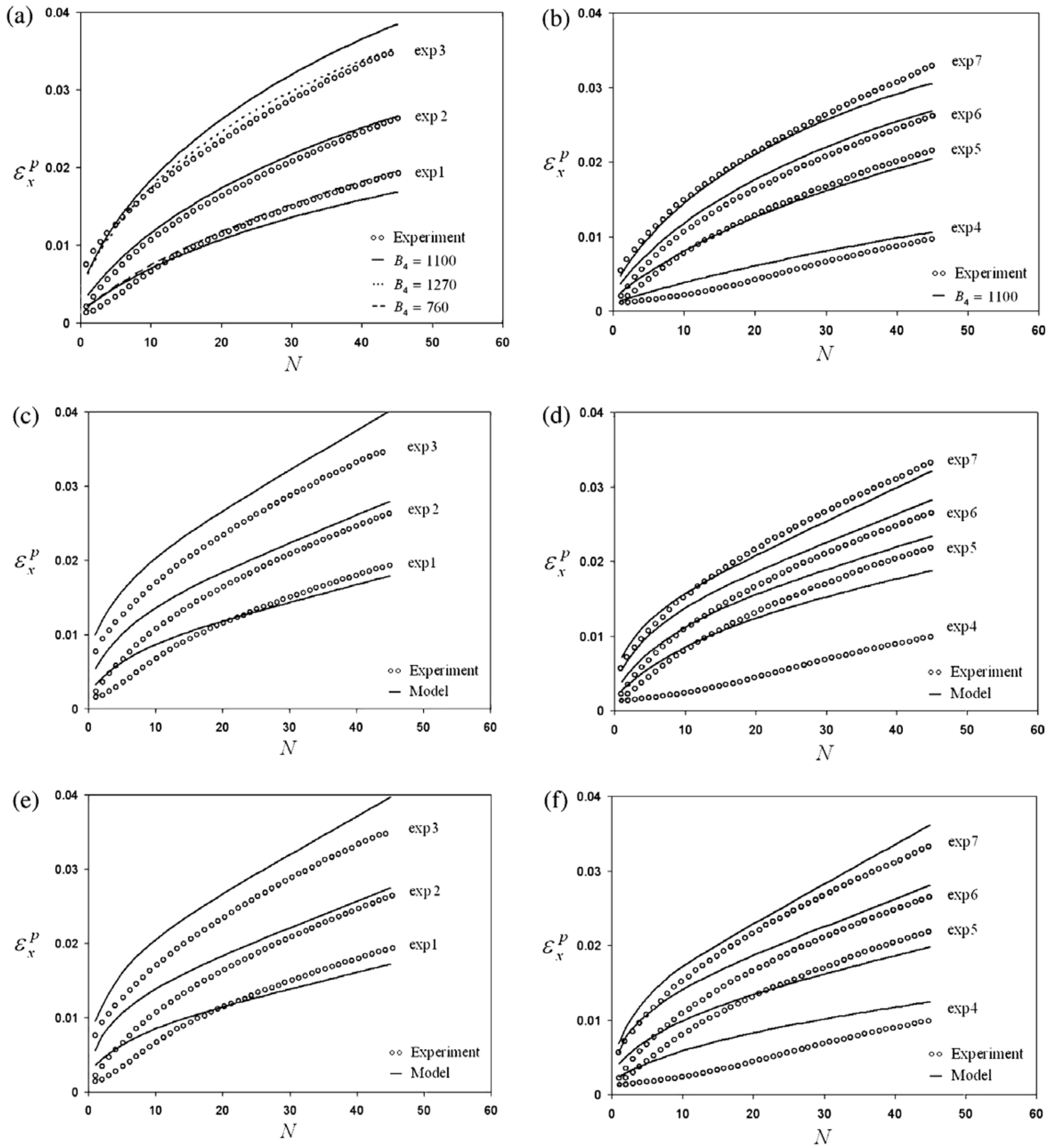

Fig. 3. Comparison of different models with experimental data from Hassan and Kyriakides (1992) for axial plastic strain at positive stress peaks. (a and b) Predictions of model N3-L1 using the material constants obtained in this paper. (c and d) Predictions of the Chaboche model using the material constants obtained by Bari and Hassan (2000). (e and f) Predictions of the Chaboche model with threshold using material constants obtained by Bari and Hassan (2000).

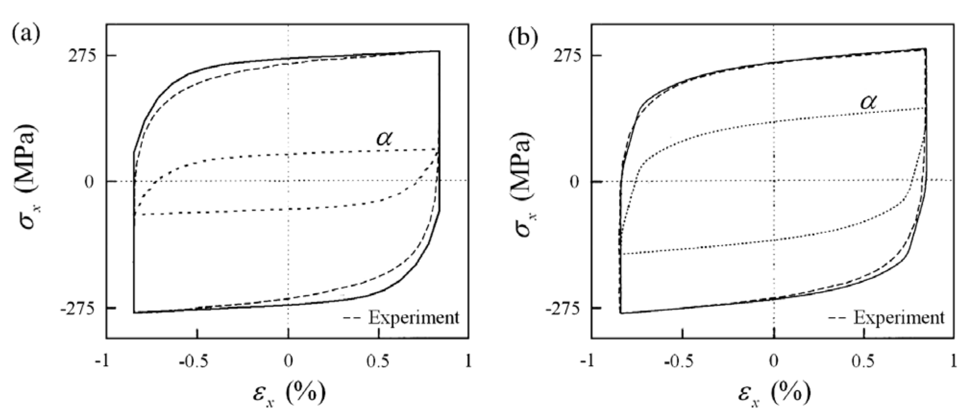

Fig. 4. Simulation of a strain controlled hysteresis loop by (a) N3-L1 and (b) C-H4T models. Data and C-H4T simulation from Bari and Hassan (2000).

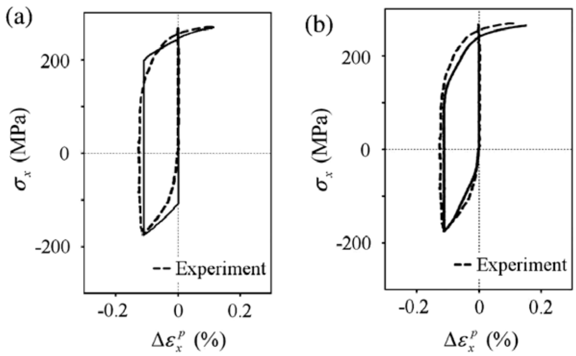

Fig. 5. Predictions of (a) N3-L1 and (b) C-H4T models for a reverse partial loading/reloading situation. Experimental data and C-H4T simulation from Bari and Hassan (2000).

for this purpose. These are also stress controlled uniaxial experiments with the loading values indicated in Table 2.

The method suggested in this paper is utilized to calibrate the Chaboche hardening model. Noting that using one linear and one nonlinear backstress components (N1-L1) produced satisfactory results, the parameter values obtained were as follows:

$$E = 173,200 \text{ MPa}, \quad \nu = 0.3, \quad \sigma_y = 324.1 \text{ MPa}$$
$$B_1 = 16,092 \text{ MPa}, \quad \gamma_1 = 35.8$$
$$B_2 = 68.9 \text{ MPa}$$

In addition, the method described by Bari and Hassan (2000) is also used for the parameter determination of the Chaboche model with threshold (C-H4T). The attained values are:

$$E = 173,200\ MPa, \quad \nu = 0.3, \quad \sigma_y = 324.1 \text{ MPa}$$
$$B_1 = 6895.8\ MPa, \quad \gamma_1 = 92.0$$
$$B_2 = 1241.1MPa, \quad \gamma_2 = 88.5$$
$$B_3 = 13,800\ MPa, \quad \gamma_3 = 89.2$$
$$B_4 = 690.0MPa, \quad \gamma_4 = 50.0, \quad \bar{a}_4 = 4.8$$

Fig. 6 shows the ratcheting prediction obtained by the above-mentioned parameters.

Table 2
Mean stress and stress amplitudes used by Hassan and Kyriakides (1992) for CS1020.

Test No.	8	9	10
σ_m (MPa)	64.1	64.1	64.1
σ_a (MPa)	331.6	337.8	351.6

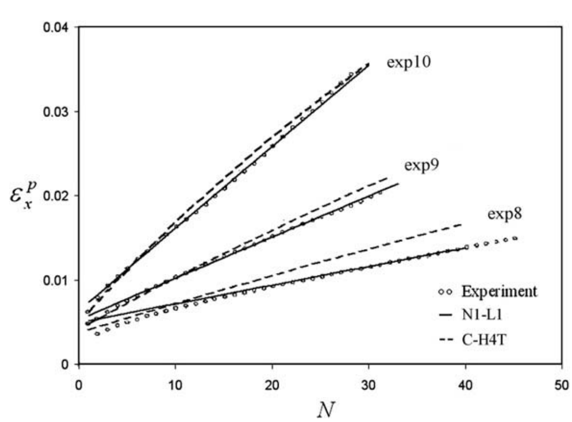

Fig. 6. Comparison of the N1-L1 and C-H4T models with experiments 8–10 from Hassan and Kyriakides (1992) conducted on CS 1020.

As can be seen in the above figure, for this set of experiments, the predictions of the Chaboche hardening model with only two components is more acceptable than the four-component Chaboche hardening model with threshold. This solely lies in the method utilized to determine the parameters of each hardening model and not in the model itself. The parameter determination method suggested by Bari and Hassan (2000) takes advantage of a stable stress–strain hysteresis curve. Since the bounding stresses of the hysteresis curve used for this example were close to the limiting stresses of exp9 and exp10, it is understandable why these experiments are better predicted by the obtained parameters. It should also be mentioned that in this method, five of the parameters ($B_2, \gamma_2, B_4, \gamma_4, \bar{a}_4$) are determined by a trial–error approach. This implies the fact that the results can be further improved, however, this would be a time consuming task.

6. Three nonlinear components and one improved attachment component (N3-A1)

As can be seen in Fig. 3, although the four-component hardening model (N3-L1) improves the ratcheting predictions, but over predicts some experiments and under predicts some other experiments. Further calculations indicate that this cannot be resolved by using more backstress components in the hardening rule. Also shown in Fig. 3a are the results of using the same parameter constants for the nonlinear components but utilizing different values of B_4 for the linear component in each experiment. These results imply the idea of employing a modified component instead of the linear attachment component used in this section.

In order to overcome the over- and under-prediction of ratcheting encountered previously (Fig. 3a), the parameter constants for the three nonlinear components of the backstress are determined in the same manner discussed in Section 4.2, but an improved definition of the forth component is introduced in the following form:

$$d\alpha_4 = \left[\frac{2}{3}C + \eta F(\beta)\right] d\varepsilon^p \tag{16}$$

where C and η are material constants and $F(\,)$ has the same form of the yield function. Tensor β can be assumed as a *virtual* backstress, with the following evolution rule:

$$d\beta = H[|F(\alpha) - F(\beta)| - \bar{a}]d\alpha \tag{17}$$

In the above equation, $\bar{a}$ is a constant scalar value and H is the Heaviside step function ($H[x] = 0$ for $x < 0$ and $H[x] = 1$ for $x \geqslant 0$). This rule indicates that whenever the distance between α and β exceeds $\bar{a}$, the evolution of the virtual backstress will be equal to the total backstress. Eq. (16) has the form of Prager's hardening rule with a varying hardening coefficient. The virtual backstress is employed only to designate the variation of this hardening coefficient and is not a component of the total backstress.

It should be stated that a quite similar approach has also been suggested by Dafalias et al. (2008), which introduced the multiplicative AF kinematic hardening rule. However, while the virtual backstress changes the value of the hardening coefficient of a Prage-type hardening rule, the multiplicative scheme essentially has its influence on the recovery term of an AF hardening rule.

Unlike the AF hardening rule where the second derivative of α_i with respect to $d\varepsilon^p$ is negative, the backstress component defined by Eqs. (16) and (17) has a positive second derivative. This might be controversial, since after some plastic flow has taken place during uniform loading, the predicted stress–strain curve would have an increasing slope. The fact is that the influence of the modified backstress component is much smaller than the sum of the other components in strain ranges encountered in ratcheting simulation or even in cyclic loadings of higher amplitudes, but when dealing with monotonic loading, the increasing tangential modulus is a rather new property. However, the primary attention of this work is towards ratcheting and the effect of using the new modified component on both monotonic and cyclic stress–strain curves will be discussed briefly, later in this section.

The values of B_i and γ_i are determined according to the method given in Section 4.2. The values of C, η and $\bar{a}$ can be evaluated by using the variation of B_4 given in Fig. 3a. For this purpose the following equation must be solved:

$$B_k = \frac{2}{3}C + \eta\left(\sqrt{\frac{3}{2}}\alpha_{xk} - \bar{a}\right) \quad (k = 1, 2, 3) \tag{18}$$

where B_k is the optimum value of B_4 for each test and α_{xk} is the maximum absolute value of the backstress for that test. In this case, the following values are obtained:

$$\begin{aligned}
&E = 181,300\ \text{MPa}, \quad \nu = 0.302, \quad \sigma_y = 186.2\ \text{MPa}\\
&B_1 = 56,330\ \text{MPa}, \quad \gamma_1 = 680.9\\
&B_2 = 8710\ \text{MPa}, \quad \gamma_2 = 841.7\\
&B_3 = 1100\ \text{MPa}, \quad \gamma_3 = 35.5\\
&C = 690\ \text{MPa}, \quad \eta = 7.78, \bar{a} = 29.6\ \text{MPa}
\end{aligned}$$

Fig. 7 shows the ratcheting predictions obtained by the new model and the above parameter values. Comparison of these results with Fig. 3 clearly indicates the accuracy of the new model in ratcheting predictions.

The result of employing the modified hardening rule in monotonic and cyclic loading is given in Fig. 8. Fig. 8a shows that the new model behaves quite similar to the N3-L1 model in a strain controlled hysteresis loop (compare to Fig. 4a). This is due to the small influence of the modified component compared to the other components of the backstress. Fig. 8b indicates that during monotonic loading, the tangent modulus increases as plastic deformations take place. This response is different from commonly used hardening rules where the slope of the stress–strain curve always decreases during plastic flow. Although it will not be studied further in this paper, but this response can be used to simulate the strain hardening phenomenon encountered in some materials after initial yielding.

7. Conclusions

A general systematic approach is established for the parameter determination of Chaboche's hardening model. The suggested method is developed through using one, two and four components of the backstress. The result of the new parameters is compared to the ones suggested by Bari and Hassan (2000). Numerical analyses indicate that if the decomposed hardening model is calibrated with this technique, the hardening rule of Chaboche can be used more efficiently than what has been credited before. After realization of the deficiency of the model, an improvement is made by applying a new formulation to one of the backstress components. The new model is demonstrated to be more precise in simulating all seven uniaxial ratcheting experiments conducted on CS 1026 by Hassan and Kyriakides (1992).

Appendix A

The multi-set nonlinear equation (Eq. (15)) encountered in Section 4.2 can be rewritten in the following form:

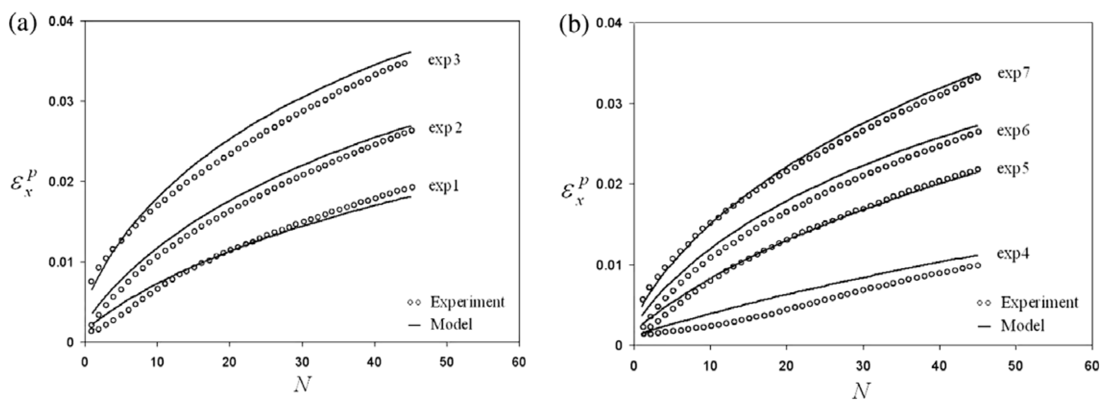

Fig. 7. Comparison of the N3-A1 model with experimental data from Hassan and Kyriakides (1992) for axial plastic strain at positive stress peaks. (a) Experiments 1–3. (b) Experiments 4–7.

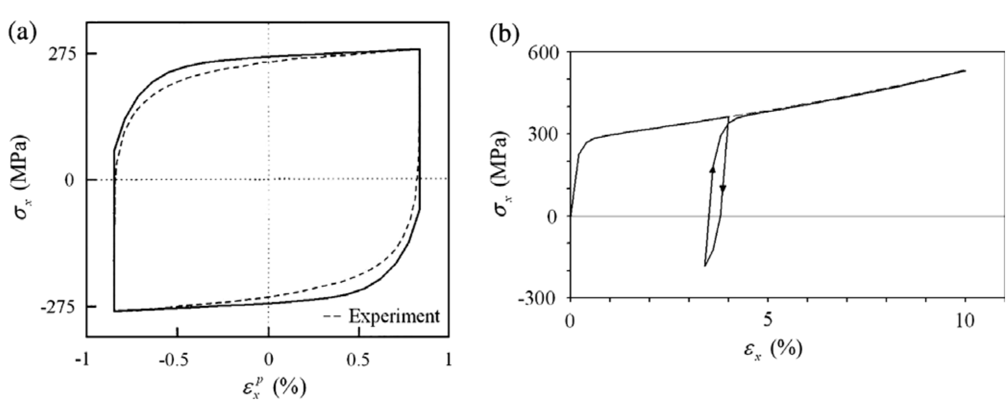

Fig. 8. Simulation of (a) strain controlled hysteresis loop and (b) monotonic stress–strain curve using the N3-A1 model.

$$C_j = \sum_i \left(A_i - A_i e^{-M_j x_i}\right) \tag{A.1}$$

As mentioned earlier in, for the solution of Eq. (A.1), the values of A_i will not be considered unknown and are predefined. Hence, the unknowns in the above set of equations are x_i which are the values of γ_i in the original equation (Eq. (15)). If three states of $C_j - M_j$ ($j = 1,2,3$) (which are actually three states of $\alpha_x - \varepsilon_x^p$) are to be satisfied by the hardening model ($j = 1,2,3$), three backstress components will be necessary for the model, therefore $i = 1,2,3$. This leads to the following set of equations:

$$\begin{cases} C_1 = A_1 - A_1 e^{-M_1 x_1} + A_2 - A_2 e^{-M_1 x_2} + A_3 - A_3 e^{-M_1 x_3} \\ C_2 = A_1 - A_1 e^{-M_2 x_1} + A_2 - A_2 e^{-M_2 x_2} + A_3 - A_3 e^{-M_2 x_3} \\ C_3 = A_1 - A_1 e^{-M_3 x_1} + A_2 - A_2 e^{-M_3 x_2} + A_3 - A_3 e^{-M_3 x_3} \end{cases} \tag{A.2}$$

The sum of A_1, A_2 and A_3 are taken to the left side of the equations and $e^{-M_1 x_i}$ is replaced with U_i, leading to:

$$\begin{cases} L_1 = A_1 U_1 + A_2 U_2 + A_3 U_3 \\ L_2 = A_1 U_1^{M_2/M_1} + A_2 U_2^{M_2/M_1} + A_3 U_3^{M_2/M_1} \\ L_3 = A_1 U_1^{M_3/M_1} + A_2 U_2^{M_3/M_1} + A_3 U_3^{M_3/M_1} \end{cases} \tag{A.3}$$

where $L_j = \sum_i A_i - C_j$ and obviously U_i ($i = 1,2,3$) are the unknowns. This equation is in a rather restricted form and may easily not have a solution. The condition $\sum A_i > |\alpha_p|, |\alpha_n|$ is a prerequisite for the existence of a solution. If the solution exists, it can be achieved by any iterative technique, for example the Newton–Raphson approach.

$$\begin{bmatrix} L_1 \\ L_2 \\ L_3 \end{bmatrix} - \begin{bmatrix} f_1 \\ f_2 \\ f_3 \end{bmatrix} = \begin{bmatrix} \partial f_1/\partial U_1 & \partial f_1/\partial U_2 & \partial f_1/\partial U_3 \\ \partial f_2/\partial U_1 & \partial f_2/\partial U_2 & \partial f_2/\partial U_3 \\ \partial f_3/\partial U_1 & \partial f_3/\partial U_2 & \partial f_3/\partial U_3 \end{bmatrix} \begin{bmatrix} \Delta U_1 \\ \Delta U_2 \\ \Delta U_3 \end{bmatrix} \begin{bmatrix} U_1 \\ U_2 \\ U_3 \end{bmatrix}_{new} = \begin{bmatrix} U_1 \\ U_2 \\ U_3 \end{bmatrix} + \begin{bmatrix} \Delta U_1 \\ \Delta U_2 \\ \Delta U_3 \end{bmatrix} \tag{A.4}$$

where:

$$\begin{aligned} f_1(U_1, U_2, U_3) &= A_1 U_1 + A_2 U_2 + A_3 U_3 \\ f_2(U_1, U_2, U_3) &= A_1 U_1^{M_2/M_1} + A_2 U_2^{M_2/M_1} + A_3 U_3^{M_2/M_1} \\ f_3(U_1, U_2, U_3) &= A_1 U_1^{M_3/M_1} + A_2 U_2^{M_3/M_1} + A_3 U_3^{M_3/M_1} \end{aligned} \tag{A.5}$$

or the more simple backward approach, which is written as:

$$\begin{aligned} U_{1(new)} &= \tfrac{1}{A_1}(L_1 - A_2 U_2 - A_3 U_3) \\ U_{2(new)} &= \left[\tfrac{1}{A_2}\left(L_2 - A_1 U_1^{M_2/M_1} - A_3 U_3^{M_2/M_1}\right)\right]^{M_1/M_2} \\ U_{3(new)} &= \left[\tfrac{1}{A_3}\left(L_3 - A_1 U_1^{M_3/M_1} - A_2 U_2^{M_3/M_1}\right)\right]^{M_1/M_3} \end{aligned} \tag{A.6}$$

Calculations have shown that a suitable starting point for the iterative solution is essential for convergence. Proper predefinition of values of A_i can also help for faster convergence. It is advised that the values of A_i not be close to each other and have the condition $L_i < A_i$.

Acknowledgement

The authors greatly acknowledge the grant provided by the Ferdowsi University of Mashhad for the financial support of this work.

References

Abdelkarim, M., Ohno, N., 2000. Kinematic hardening model suitable for ratcheting with steady-state. International Journal of Plasticity 16, 225–240.

Armstrong, P.J., Frederick, C.O., 1966. A mathematical representation of the multiaxial Bauscinger effect. Cegb Report No. Rd/B/N 731.

Aubin, V., Quaegebeur, P., Degallaix, S., 2003. Cyclic plasticity of a duplex stainless steel under non-proportional loading. Material Science and Engineering A 346, 208–215.

Bari, S., Hassan, T., 2000. Anatomy of coupled constitutive models for ratcheting simulation. International Journal of Plasticity 16, 381–409.

Bari, S., Hassan, T., 2002. An advancement in cyclic plasticity modeling for multiaxial ratcheting simulation. International Journal of Plasticity 18, 873–894.

Benham, P.P., 1965. Some observations on the cyclic strain-induced creep in mild steel at room temperature. International Journal of Mechanical Sciences 7, 81–86.

Benallal, A., Le Gallo, P., Marquis, D., 1989. An experimental investigation of cyclic hardening of 316 stainless steel and of 2024 aluminum alloy under multiaxial loading. Nuclear Engineering and Design 114, 345–353.

Besseling, J.F., 1958. A theory of elastic, plastic, and creep deformations of an initially isotropic material. ASME Journal of Applied Mechanics 25, 529–536.

Bocher, L., Delobelle, P., Robinet, P., Feaugas, X., 2001. Mechanical and microstructural investigations of an austenitic stainless steel under non-proportional loadings in tension–torsion-internal and external pressure. International Journal of Plasticity 17, 1491–1530.

Chaboche, J.L., Dang-Van, K. Cordier, G., 1979. Modelization of strain memory effect on the cyclic hardening of 316 stainless steel. In: Transactions of the 5th International Conference on Structural Mechanics in Reactor Technology, Berlin, No. Div L in 11/3.

Chaboche, J.L., 1986. Time-independent constitutive theories for cyclic plasticity. International Journal of Plasticity 2, 149–188.

Chaboche, J.L., 1991. On some modifications of kinematic hardening to improve the description of ratcheting effects. International Journal of Plasticity 7, 661–678.

Chaboche, J.L., 2008. A review of some plasticity and viscoplasticity constitutive theories. International Journal of Plasticity 24, 1642–1693.

Chen, X., Jiao, R., 2004. Modified kinematic hardening rule for multiaxial ratcheting prediction. International Journal of Plasticity 20, 871–898.

Chen, X., Jiao, R., Kim, K.S., 2005. On the Ohno–Wang kinematic hardening rules for multiaxial ratcheting modeling of medium carbon steel. International Journal of Plasticity 21, 161–184.

Colak, O.U., 2008. Kinematic hardening rules for modeling uniaxial and multiaxial ratcheting. Materials and Design 29, 1575–1581.

Corona, E., Hassan, T., Kyriakides, S., 1996. On the performance of kinematic hardening rules in predicting a class of biaxial ratcheting histories. International Journal of Plasticity 12, 117–145.

Dafalias, Y.F., Kourousis, K.I., Saridis, G.J., 2008. Multiplicative AF kinematic hardening in plasticity. International Journal of Solids and Structures 45, 2861–2880.

Dafalias, Y.F., Popov, E.P., 1974. A model of nonlinearly hardening materials for complex loading. In: Proceedings of the 7th US National Congress of Theoretical and Applied Mechanics (Abstract), Boulder, Colorado, June 1974, p. 149.

Dafalias, Y.F., Popov, E.P., 1975. A model of nonlinearly hardening materials for complex loading. Acta Mechanica 21, 173–192.

Dafalias, Y.F., Popov, E.P., 1976. Plastic internal variables formalism of cyclic plasticity. ASME Journal of Applied Mechanics 43, 645–650.

Dafalias, Y.F., 1986. Bounding surface plasticity. Part I: mathematical foundation and hypoplasticity. ASCE Journal of Engineering Mechanics 112, 966–987.

Delobelle, P., Robinet, P., Bocher, L., 1995. Experimental study and phenomenological modelization of ratcheting under uniaxial and biaxial loading on an austenitic stainless steel. International Journal of Plasticity 11, 295–330.

Freudenthal, A.M., Ronay, M., 1966. Second order effects in dissipative media. Proceedings of the Royal Society A 294, 14–50.

Hassan, T., Corona, E., Kyriakides, S., 1992. Ratcheting in cyclic plasticity, part II: multiaxial behavior. International Journal of Plasticity 8, 117–146.

Hassan, T., Kyriakides, S., 1992. Ratcheting in cyclic plasticity, part I: uniaxial behavior. International Journal of Plasticity 8, 91–116.

Hassan, T., Kyriakides, S., 1994a. Ratcheting of cyclically hardening and softening materials, part I: uniaxial behavior. International Journal of Plasticity 10, 149–184.

Hassan, T., Kyriakides, S., 1994b. Ratcheting of cyclically hardening and softening materials, part II: multiaxial behavior. International Journal of Plasticity 10, 185–212.

Hassan, T., Taleb, L., Krishna, S., 2008. Influence of non-proportional loading on ratcheting responses and simulations by two recent cyclic plasticity models. International Journal of Plasticity 24, 1863–1889.

Jiang, Y., Sehitoglu, H., 1996. Modeling of cyclic ratchetting plasticity, part I: development of constitutive relations. ASME Journal of Applied Mechanics 63, 720–725.

Kang, G.Z., Gao, Q., Yang, X.J., 2004. Uniaxial and nonproportional multiaxial ratchetting of SS304 stainless steel at room temperature: Experiments and simulations. International Journal of Non-Linear Mechanics 39, 843–857.

Koo, G.H., Lee, J.H., 2007. Investigation of ratcheting characteristics of modified 9Cr–1Mo steel by using the Chaboche constitutive model. International Journal of Pressure Vessels and Piping 84, 284–292.

Krieg, R.D., 1975. A practical two-surface plasticity theory. ASME Journal of Applied Mechanics 42, 641–646.

Mcdowell, D.L., 1995. Stress state dependence of cyclic ratcheting behavior of two rail steels. International Journal of Plasticity 11, 397–421.

Moyar, G.J., Sinclair, G.M., 1963. Cyclic strain accumulation under complex multiaxial loading. In: Proceedings of the Joint International Conference on Creep. Institution of Mechanical Engineers, London, pp. 2–47.

Mroz, Z., 1967. On the description of anisotropic work hardening. Journal of Mechanics and Physics of Solids 15, 163–175.

Ohno, N., Wang, J.D., 1993. Kinematic hardening rules with critical state of dynamic recovery, part I: formulations and basic features for ratcheting behavior. International Journal of Plasticity 9, 375–390.
Portier, L., Calloch, S., Marquis, D., Geyer, P., 2000. Ratchetting under tension–torsion loadings: experiments and modeling. International Journal of Plasticity 16, 303–335.
Prager, W., 1956. A new method of analyzing stresses and strains in work hardening plastic solids. Journal of Applied Mechanics 23, 493–496.
Ruiz, C., 1967. High-strain fatigue of stainless-steel cylinders: experimental results and their application to pressure–vessel design. Journal of Strain Analysis 2, 290.
Voyiadjis, G.Z., Basuroychowdhury, I.N., 1998. A plasticity model for multiaxial cyclic loading and ratchetting. Acta Mechanica 126, 19–35.
Yoshida, F., 1995. Ratcheting behavior of 304 stainless steel at 650 °C under multiaxial strain-controlled and uniaxailly/multiaxially stress-controlled conditions. European Journal of Mechanics-A/Solids 14, 97–117.
Yoshida, F., Tajima, N., Ikegami, K., Shiratori, E., 1978. Plastic theory of the mechanical ratcheting. Bulletin of the JSME 21, 389–397.